Plant Mol Biol (2017) 94:319–332
DOI 10.1007/s11103-017-0609-5

Genomic and functional characterization of coleopteran insect-specific α-amylase inhibitor gene from Amaranthus species

Amey J. Bhide[1] · Sonal M. Channale[1] · Yashpal Yadav[1] · Kabita Bhattacharjee[1] · Pankaj K. Pawar[2] · V. L. Maheshwari[3] · Vidya S. Gupta[1] · Sureshkumar Ramasamy[1] · Ashok P. Giri[1]

Received: 14 September 2016 / Accepted: 31 March 2017 / Published online: 12 April 2017

Abstract The smallest 32 amino acid α-amylase inhibitor from *Amaranthus hypochondriacus* (AAI) is reported. The complete gene of pre-protein (*AhAI)* encoding a 26 amino acid (aa) signal peptide followed by the 43 aa region and the previously identified 32 aa peptide was cloned successfully. Three cysteine residues and one disulfide bond conserved within known α-amylase inhibitors were present in AhAI. Identical genomic and open reading frame was found to be present in close relatives of *A. hypochondriacus* namely *Amaranthus paniculatus, Achyranthes aspera* and *Celosia argentea*. Interestingly, the 3′UTR of *AhAI* varied in these species. The highest expression of *AhAI* was observed in *A. hypochondriacus* inflorescence; however, it was not detected in the seed. We hypothesized that the inhibitor expressed in leaves and inflorescence might be transported to the seeds. Sub-cellular localization studies clearly indicated the involvement of AhAI signal peptide in extracellular secretion. Full length rAhAI showed differential inhibition against α-amylases from human, insects, fungi and bacteria. Particularly, α-amylases from *Helicoverpa armigera* (Lepidoptera) were not inhibited by AhAI while *Tribolium castaneum* and *Callosobruchus chinensis* (Coleoptera) α-amylases were completely inhibited. Molecular docking of AhAI revealed tighter interactions with active site residues of *T. castaneum* α-amylase compared to *C. chinensis* α-amylase, which could be the rationale behind the disparity in their IC_{50}. Normal growth, development and adult emergence of *C. chinensis* were hampered after feeding on rAhAI. Altogether, the ability of AhAI to affect the growth of *C. chinensis* demonstrated its potential as an efficient bio-control agent, especially against stored grain pests.

Keywords α-Amylase · α-Amylase inhibitor · *Amaranthus hypochondriacus* · *Tribolium castaneum* · *Callosobruchus chinensis* · Signal peptide

Introduction

A constant molecular battle exists between host plants and their insect pests. Plants synthesize various defensive proteins including inhibitors against insect digestive enzymes (Ambekar et al. 1996; Giri and Kachole 1998) while insects overcome the digestive inhibition by producing multiple isoforms of these enzymes having differential sensitivity (Zavala et al. 2008; Sarate et al. 2012). Insect digestive α-amylases play an important role in digestion and assimilation of starch and carbohydrates ingested by feeding on host plants (Franco et al. 2002). Plants, on the contrary, produce various proteinaceous α-amylase inhibitor (α-AI) and protease inhibitors in response to insect feeding (Franco et al. 2002; Mishra et al. 2012). Monomeric, dimeric and tetrameric α-AIs from wheat and barley have been studied extensively and particularly against storage insect pests (Petrucci et al. 1976; Lazaro et al. 1988;

Electronic supplementary material The online version of this article (doi:10.1007/s11103-017-0609-5) contains supplementary material, which is available to authorized users.

✉ Ashok P. Giri
ap.giri@ncl.res.in

[1] Plant Molecular Biology Unit, Division of Biochemical Sciences, CSIR-National Chemical Laboratory, Dr. Homi Bhabha Road, Pune 411 008, India

[2] Department of Biochemistry, Shivaji University, Kolhapur 416 004, India

[3] School of Life Sciences, North Maharashtra University, Jalgaon 425 001, India

Sanchez-Monge et al. 1986; Gomez et al. 1989). Similarly, α-AIs from rice, castor seeds and water jasmine were also evaluated for effective inhibition of insect digestive enzymes (Yamasaki et al. 2006; Do Nascimento et al. 2011; Nguyen et al. 2014). α-AI lectins were shown to affect normal growth and physiology of insect pests (Paes et al. 2000; Napoleao et al. 2012; Lagarda-Diaz et al. 2014). Various transgenic plants carrying heterologous α-AI have demonstrated effectively in mitigating insect infestation (Pereira et al. 1999; Luthi et al. 2013).

Detailed analysis of molecular interactions between plant α-AI and insect digestive α-amylases is essential to design potent and effective inhibitors (Giri et al. 2004, 2016). Molecular insights of the underlying inhibitory mechanism of α-AI were studied through three-dimensional structures of enzyme-inhibitor complexes. Basic interaction of the α-AI with α-amylases involved specific hydrogen bonding interaction between the amino acid residue of the inhibitory loop and active sites of the enzyme (Chagolla-Lopez et al. 1994; Pereira et al. 1999). Precise hydrogen bonding of arginine, tyrosine and tryptophan residues present on an inhibitory loop of microbial α-AI, Tendamistat and active site residues of porcine pancreatic α-amylase was reported (Wiegand et al. 1995). Significant variation in conformational changes observed in the inhibitory loop of *Phaseolous vulgaris* α-AI upon binding to insect and mammalian α-amylases was suggested as an underlying mechanism for the differential inhibitory activity (Nahoum et al. 1999). Similarly, a distinct mode of interaction between wheat α-AI and α-amylase isoforms from *Helicoverpa armigera* was detected. Aggregation of one of the isoforms with wheat α-AI was predicted to be responsible for its respective higher inhibition (Bhide et al. 2015).

Much of the knowledge of inhibitory mechanism has come from the analysis of effects of various mutations in the inhibitory domain(s) of a particular inhibitor on its inhibitory activity. For example, peptide variants of proteinaceous α-AI from *Tephrosia villosa* (TvD1) were generated through in vitro mutagenesis and the effect of mutations on its overall inhibitory activity was studied (Liu et al. 2006; Lin et al. 2007; Vijayan et al. 2012). A mechanism of steric hindrance was observed for bifunctional α-AI (BASI) from barley which inhibits endogenous α-amylases by binding to active site of the enzyme. In this case, an unusual completely solvated calcium ion was located at the protein–protein interface (Vallee et al. 1998). Different types of α-AI were also reported to possess proteolytic and chitinolytic activities along with the amylolytic activity (Strobl et al. 1998; Dayler et al. 2005).

α-AIs have various applications in medicine and fermentation industries. For example, barley α-AI was found to be industrially important as it was involved in improving beer foam stability during processing (Limure et al. 2015). Moreover, α-AI also has positive effects on cancer progression. Additionally, micro-RNA-mediated β-catenin signalling was targeted by barley BASI which eventually impeded glioblastoma progression (Shi et al. 2014). Information regarding induction and regulation of various α-AI expressions under different stress conditions is limited. However, a report suggests the synthesis of α-AI could be induced by abscisic acid and dehydration stress (Robertson et al. 1989). In the present study, a *α-AI* gene from *Amaranthus hypochondriacus* (*AhAI*) was characterized at molecular and biochemical levels. Although the interaction of AhAI with various α-amylases from bacterial, fungal, mammalian and lepidopteran insect showed moderate or no inhibition, coleopteran insect α-amylases were strongly inhibited by the same. Further, AhAI's potential for in vivo suppression of growth and development of stored grain pest *Callosobruchus chinensis* was also investigated.

Materials and methods

Sequence and phylogenetic analysis of α-amylase inhibitors

Full-length amino acid sequences of all the α-AIs were extracted from NCBI database. Multiple sequence alignment of these sequences was carried out using Clustal Omega and the Neighbor-joining (NJ) tree was generated by MEGA6 (Tamura et al. 2013) using 1000 bootstrap replicates, and fungal (*Streptomyces avermitilis*) α-AI (GenBank accession No. ACU45382.1) as an out-group. Multiple sequence alignment of AhAI and other α-AIs was performed using Clustal Omega and secondary structural features were evaluated and highlighted using online software EsPript3 (Robert and Gouet 2014).

RNA isolation, cDNA synthesis and qPCR

Total RNA was extracted from young and mature leaves, young and mature inflorescence and seeds of *Amaranthus hypochondriacus, A. paniculatus, Celosia argentea* and *Achyranthes aspera* using Trizol reagent (Invitrogen, CA, USA). Crude RNA samples were treated with RQ1 DNase (Promega, USA). Two microgram of the DNA-free RNA samples was reverse-transcribed using oligo dT primers and reverse transcriptase (Promega, USA) as per the manufacturer's recommendations. qPCR primer pairs were designed in non-homologous regions of α-AI (Table S1). cDNA was diluted before use in a PCR reaction and quantitative q PCR reactions were performed using AB 7900 Fast Start q PCR System (Applied Biosystems, USA; cycler conditions: 95 °C for 10 min; 40 cycles of 3 s at 95 °C and 30 s at 55 °C with an additional dissociation stage of 15 s

each at 95, 55 and 95 °C) and SYBR Green PCR master mix (Roche Applied Science, Germany). Each plate was run with a standard curve and no template control. Relative quantification was carried out using the standard curve method with Elongation Factor 1α (EF1α) as a reference gene (Table S1). Amplification efficiency of each gene was assessed by plotting a standard curve using five serial dilutions of cDNA from a template pool and similar efficiencies were calculated by LinRegPCR software (http://www.hartfaalcentrum.nl/index.php). The target gene expression levels were then normalized using EF1α.

Sequence analysis of 3′UTR region

RNA was isolated and cDNA was prepared from young leaves of *A. hypochondriacus*. Degenerate primers were designed and amplified PCR products (~100 bp) were cloned into pGEM-T vector (Promega, USA) and sequenced. 5′ and 3′ sequence ends were amplified as per manufacturer's instructions (Clontech, USA) and resulted products were sequenced to obtain full-length nucleotide sequence of the inhibitor. Sequenced 3′UTR regions of various full-length *AhAI* transcripts from *A. hypochondriacus* and its related species *viz. A. paniculatus, A. aspera, C. argentea* were aligned using clustal Omega.

Cloning, expression and purification of *AhAI*

Open reading frame (ORF) of AhAI (GenBank accession: KU641477) without the native signal peptide of 26 amino acids (aa) was amplified using designed primer pairs (Table S1) and cloned in pET 28-a expression vector (Novagen, Madison, USA) in frame with N-terminus 6X His-tag. Recombinant plasmids were amplified and transformed into *Escherichia coli* BL21 Star (DE3) cells. BL21 cells transformed with *AhAI* constructs were induced with 0.54 mM isopropyl-β-D-1-thiogalactopyranoside (IPTG) and incubated at 37 °C for 5 h. AhAI protein was purified from inclusion bodies using on-column refolding method (Oganesyan et al. 2005). In brief, cell lysis was performed in the lysis buffer (50 mM HEPES, pH 7.0, 100 mM NaCl) by sonication (5 min with 45% amplitude, alternating 8 s on; 12 s off cycles) on ice followed by centrifugation at 8000 rpm for 20 min. The pellet was washed in same buffer containing 1 M Urea, 2% Triton X-100. Further, pellet was solubilized in the denaturing buffer (20 mM Tris pH 8.5, 8 M Urea, 100 mM NaCl, 1 mM β-mercaptoethanol) by gentle vortex at room temperature. The solubilized protein from inclusion bodies was bound to Ni–NTA pre-equilibrated resin at room temperature overnight. On-column refolding was achieved with different buffers (10 column volumes of each buffer) under gravity. All the working solutions were prepared in Buffer-A (20 mM Tris, pH 8.5, 100 mM NaCl). First, column was washed with denaturing buffer containing 10 mM imidazole followed by buffer A containing 0.1% Triton X-100 and 500 mM NaCl. The column was further washed with buffer A containing 5 mM cyclodextrin followed by another wash with buffer A. The protein was eluted with buffer A containing 500 mM imidazole and 10% glycerol.

Eluted fractions of AhAI were pooled and subjected to buffer exchange (20 mM Tris, pH 8.5, respectively) by passing through 3 kDa cut-off column (Millipore, Billerica, USA). Protein was quantified by Bradford assay (Bio-Rad, USA) using BSA as a standard. Purified proteins were loaded on 12% SDS–PAGE to check the purity of samples.

Localization of GFP fused with AhAI signal peptide

CDS of GFP was amplified using designed long primer containing complete nucleotide sequence of AhAI signal peptide (Table S1). Both signal peptide with GFP (SP-GFP) and only GFP sequence were cloned in binary plant expression vector pRI101-AN (Takara Bio Inc., Japan). Constructs pRI101-AN:SP:GFP and pRI101-AN:GFP were electroporated into *Agrobacterium tumefaciens* strain GV3101 using a standard electroporation protocol. Empty pRI101-AN vector was used as a negative control. Cultures of *A. tumefaciens* GV3101 containing respective constructs were grown at 28 °C in Luria–Bertani medium containing selection markers (25 µg/mL rifampicin and 50 µg/mL kanamycin) at 120 rpm for 24 h. Agrobacterium cells were harvested by centrifugation at 3500 rpm for 5 min and suspended in infiltration buffer (half strength MS medium, pH 5.6, Hi-Media, India and 200 µM acetosyringone). Agrobacterium cells were pelleted and resuspended in infiltration buffer by adjusting an OD 1.0 at 600 nm. Cultures were incubated at 24 °C for 3 h before infiltration. After incubation, Agrobacterium cultures were infiltrated into the leaves of 2 weeks old *Nicotiana benthamiana* seedlings. Plants were maintained at 24 °C in a growth chamber. Leaf sections were visualized for sub-cellular localization of GFP using confocal scanning microscope (Zeiss LSM 710, Germany) at 4 dpi after agro-infiltration.

Extraction of apoplastic fluid and western blot analysis

Apoplastic fluid from tobacco leaves was extracted 4 days post-agro-infiltration as described by O'Leary et al., (2014). Briefly, syringe method was used to create a negative pressure inside the barrel containing leaves to infiltrate 20 mM phosphate buffer (pH 7.0) inside leaves. Leaves after infiltration were carefully blotted and rolled around the 1 mL tip and were inserted inside the small syringe barrel. Barrel was kept inside the 50 mL centrifuge tube and the whole assembly was centrifuged at 800 rpm for 10 min.

Care was taken not to cause any injury to leaves throughout the process as it may lead to leak intracellular content into the apoplastic extract. Collected apoplastic extract was concentrated through 3 kDa cut-off column and protein was quantified by Bradford method. An equal quantity of protein (28 µg) from apoplastic fluid and the remaining tissue was loaded on 12% SDS-PAGE gel. After running the gel, protein was transferred to PVDF membrane. Gel was stained with silver stain to ensure the complete transfer. Standard western blot protocol was followed using primary rabbit anti-GFP polyclonal antibodies (Abcam, Cambridge, UK) at 1:3000 dilution and secondary anti-rabbit goat polyclonal antibodies (Santa Cruz Biotechnology, Inc., USA) at 1:7000 dilution. Recombinant GFP protein was also loaded and detected as a positive control.

Determination of accurate molecular weight and α-amylase inhibitory activity

AhAI (4.0 mg/mL) was mixed with sinapinic acid (Sigma–Aldrich, St Louis, USA) (50% CAN, 0.1% TFA) in 1:5 ratio. About 0.5 µL of this mixture was spotted on the MALDI target plate by dry droplet method. The mass spectral analysis was done on AB SCIEX MALDI-TOF/TOF^{TM}5800 system. Positive linear mode was used as a mode of operation. MS data were acquired at a laser repetition rate of 400 Mz with 1000 laser shots per spectrum over each sample spot in the range of 5.0–20 kDa for AhAI.

All the assays of α-amylase activity were performed by monitoring liberation of reducing sugars from starch using DNSA (Dinitrosalicylic acid) reagent. A premix of triplicate reactions was prepared in respective buffers and equal units of purified recombinant enzyme (determined by adjusting the absorbance at 0.5 at 540 nm as described earlier; Bhide et al. 2015; Channale et al. 2016) to which 150 µL of starch (0.25%) was added. After 15 min of incubation at 37 °C, the reaction was stopped by adding 500 µL of DNSA reagent and reaction tube was incubated in boiling water bath for 5 min and absorbance was measured at 540 nm. One α-amylase unit was defined as the amount of enzyme required to release 1 µM maltose/min at 37 °C from the substrate (starch) under the given assay conditions.

Insect rearing and feeding assay

C. chinensis culture was obtained from Entomology department, CSIR-NCL, Pune. Freshly emerged *C. chinensis* adults were transferred to uninfected mung bean seeds and culture was maintained by transferring concurrent generations on fresh seeds. The cultures were maintained under controlled conditions at 25 °C, 65% relative humidity with 12 h each dark and light cycle in insect growth chamber.

The effect of recombinant α-AI on the growth of *C. chinensis* was studied by treating mung bean seeds with α-AI at 0 (control), 10.0, 25.0 µM concentration prepared in 20 mM Tris pH 8.5, 10% glycerol and 100 mM NaCl. For α-AI treatment, 50 mung bean seeds were soaked in the above-mentioned concentration of α-AI for 60 min. The seeds were air-dried for 4 h. Five pairs of freshly emerged insects were allowed to lay eggs on the mung bean seeds; the insects were then separated from mung bean seeds after 72 h. The eggs were counted after 7 days of oviposition (Wisessing et al. 2010). The seeds were monitored and adults were counted after their emergence. Total weight of emerged adults was recorded and the percentage of adults emerged was calculated (Table S2).

Circular-Dichroism spectroscopy and homology modeling of AhAI

Circular-Dichroism (CD) assays were carried out using Jasco J-815 spectropolarimeter (Jasco, Tokyo, Japan) under constant nitrogen flow equipped with a Peltier-type temperature cuvette holder. Far-UV spectra were recorded using 0.1 cm path length quartz cuvette. Buffer conditions for purified AhAI (at a final concentration of 50 µg/mL) were exchanged to 20 mM Tris pH 8.5 to remove residual imidazole. Three consecutive measurements were accumulated to obtain mean spectra. The observed ellipticities were converted into molar ellipticities (θ) based on molecular mass per residue of AhAI. Percentage of secondary structures was calculated using CD-Pro software (http://sites.bmb.colostate.edu/sreeram/CDPro/).

Homology modeling of 75 aa AhAI was performed by submitting protein sequence to I-TASSER server (http://zhanglab.ccmb.med.umich.edu/I-TASSER/). A model was selected out of five predicted models based on CD spectroscopic data (Fig. S1). A separate motif analysis for 43 aa sequence was performed using Prosite server (http://prosite.expasy.org/).

Docking studies of AhAI with CcAmy and TcAmy

The three-dimensional structures of CcAmy and TcAmy were predicted using MODELLER ver.9.15 (Sali and Blundell 1993; Webb and Sali 2014). The crystal structure of *Tenebrio molitor* α-amylase (PDB ID: 1JAE, Strobl et al. 1998) was used as a template. The models were evaluated on the basis of the lowest discrete optimized protein energy (DOPE) score. The structural assessment of the models was performed using RAMPAGE (Lovell et al. 2003). The visualization of the above models was performed using Pymol (https://www.pymol.org ; DeLano Scientific LLC, USA).

Prediction of AhAI inhibitor binding with CcAmy and TcAmy was carried out using docking studies.

Corresponding residues belonging to the inhibitor binding site, in the TmAmy structure (1TMQ) were correlated. The web-based protein–protein docking program GRAMM-X with default parameters was used for docking of proteinaceous AhAI inhibitor with CcAmy and TcAmy (Tovchigrechko and Vakser 2006).

Results

Gene structure and comparison of *AhAI* with other α-amylase inhibitors

A 32 aa long mature peptide showing α-AI activity was reported in the literature. The peptide was purified from Amaranth seeds, aa sequence was deduced by Edman degradation and structure was determined by NMR (Chagolla-Lopez et al. 1994; Lu et al. 1999). In the present study, complete DNA sequence (CDS) of *AhAI* was elucidated by amplifying cDNA ends. *AhAI* gene had signal peptide of 26 aa followed by 43 aa long region along with reported mature peptide of 32 aa (Fig. 1a). Biochemical or molecular function could not be assigned to internal fragment. A possible mechanism for in vivo cleavage of an internal fragment from mature peptide also remains unclear. Phylogenetic analysis of AhAI protein with known α-AIs from eudicots and monocots indicated a strict phylogenetic differentiation of AhAI from monocot (Fig. 1b). A similar α-AI showing 53% identity with AhAI was deposited from *B. vulgaris* (GenBank accession No. XP_010672947.1). This α-AI showed unique secondary structural identity with AhAI (Fig. 1c). Structural alignment with other α-AIs showed conservation of three cysteine residues and single disulfide bond across AhAI secondary structure (Fig. 1d). This conserved disulfide bond is crucial in maintaining characteristic disulfide topology of knottin-type α-AI.

AhAI orthologs from Amaranthaceae members exhibit identical ORF and variation in 3′UTR sequence

One domestic and two wild relatives of *A. hypochondriacus viz. A. paniculatus, Celosia argentea* and *Achyranthes aspera*, respectively, were found to contain identical nucleotide sequence of *AhAI* ORF. Interestingly, genomic regions within this sequence of α-AI were namely indistinguishable. However, various *AhAI* transcript sequences (clones) from these four species showed variation in their 3′UTR regions (Fig. 2). Polyadenylation recognition site was identified in all of the transcripts. 3′UTR region was known to possess sites for binding of microRNAs (miRNAs) which play an important role in the regulation of translation of desired protein (Bartel 2009). In silico analysis of *AhAI* 3′UTR region did not show any possible miRNAs binding sites and had found no evidence for alternate splicing.

AhAI transcript abundance varies across the plant tissues of candidate Amaranthaceae members

Relative transcript abundance was analyzed in various plant parts from one domestic and two wild relatives of *A. hypochondriacus viz. A. paniculatus, C. argentea* and *A. aspera*, respectively. *AhAI* transcripts were abundant in *A. hypochondriacus* tissues specifically in inflorescence as compared to the plant tissues from other species. Although abundant α-AI protein was found in *A. hypochondriacus* seeds (Chagolla-Lopez et al. 1994), in our study *AhAI* transcripts remained undetectable in the seeds of all four species. All selected members showed variation in transcript abundance within respective plant tissues viz. young leaves, mature leaves, young inflorescence, mature inflorescence and seeds (Fig. 3). *A. hypochondriacus* mature inflorescence showed 40-fold higher expression of *AhAI* transcripts compared to young leaves whereas *A. paniculatus* and *C. argentea* had only twofold higher expression in their mature inflorescence. In contrast, *AhAI* transcript abundance in the mature inflorescence of *A. aspera* was one-third of that in young leaves. Similarly, when compared within respective plant tissues, *AhAI* transcripts were higher in the mature inflorescence of all three species except in *A. aspera* where mature leaves indicated the highest *AhAI* expression. Overall, AhAI protein was reported only from *A. hypochondriacus* seeds, transcripts were found in various plant tissues of four relative Amaranthaceae species. Moreover, *AhAI* transcript abundance varied within plant tissues and across the four relative species.

AhAI signal peptide mediates extracellular transport

Although AhAI protein was reported earlier to present abundantly in *A. hypochondriacus* seeds, *AhAI* transcripts in *A. hypochondriacus* seeds were undetectable (Fig. 3). Hence, AhAI synthesized in leaves or inflorescence could be transported to the seeds. Functional analysis of AhAI signal peptide was carried out to understand its possible role in extracellular transport. The signal peptide was fused to GFP and agro-infiltrated into the young tobacco leaves. Transiently expressed GFP protein without signal peptide was prominently observed in nucleus, cytoplasm and periphery, while GFP protein fused with AhAI signal peptide was observed only at the periphery and in extracellular spaces of the plant cell known as apoplast (Fig. 4a). GFP protein was not visible either in the nucleus or in the cytoplasm when fused with AhAI signal peptide. To support the above findings, apoplastic fluid was extracted and extracellularly secreted GFP protein

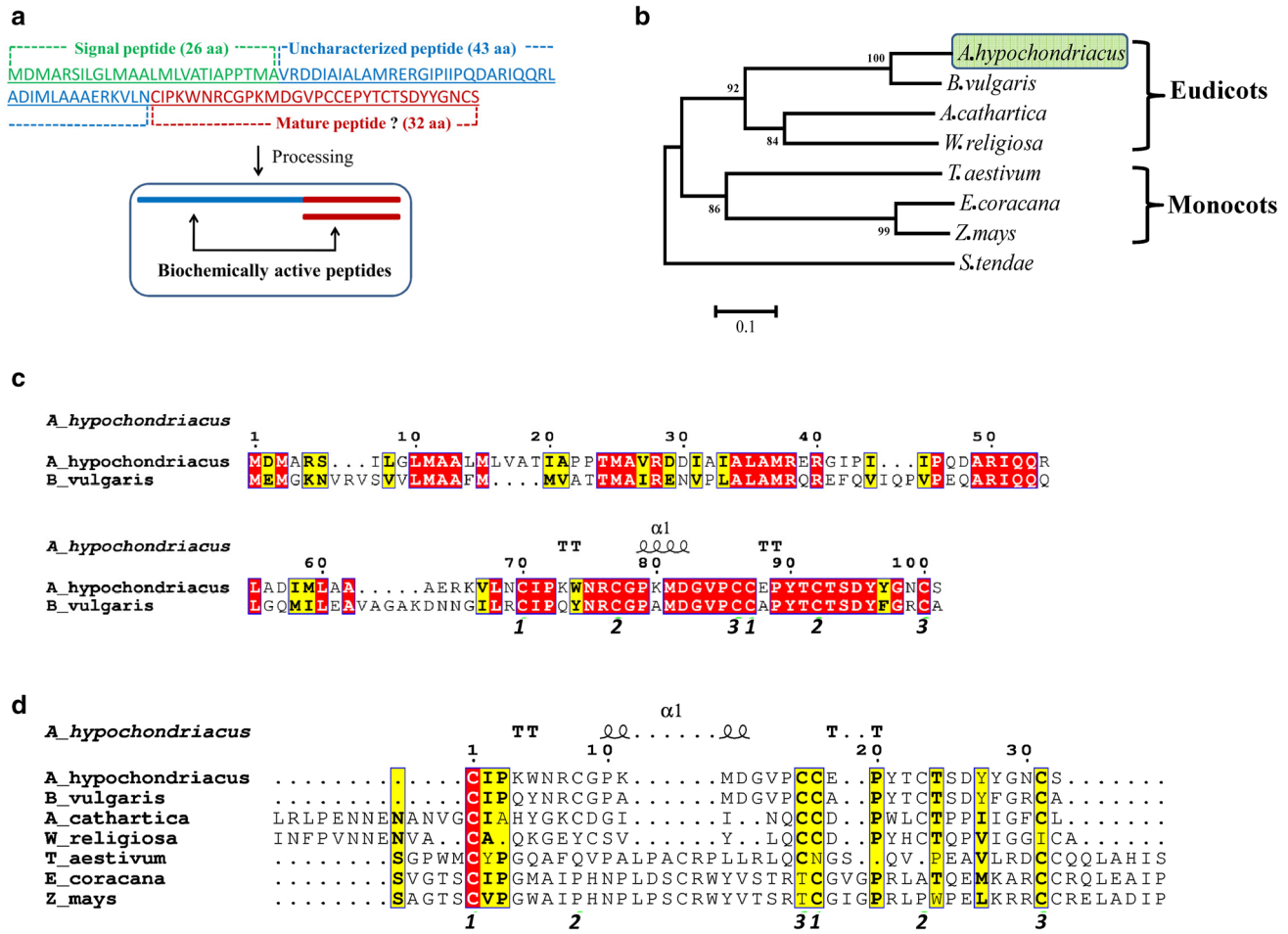

Fig. 1 Comparison of AhAI protein sequence with known plant α-amylase inhibitors **a** Schematic representation of *AhAI* transcript. **b** Amino acid sequence divergence of plant α-AI. Cladogram with protein sequences was constructed using MEGA 6 software and Neighbor-Joining method with 1000 iterations. Fungal (*Streptomyces tendae*) α-AI (GenBank accession No. AAA26686.1) was used as an out-group. **c** Structure based sequence alignment of AhAI with putative *Beta vulgaris* α-AI (GenBank accession No. XP_010672947.1). Multiple sequence alignment was performed using Clustal Omega. The secondary structure elements above the sequence blocks correspond to the reported crystal structure of Amaranth α-AI (AAI; PDB ID: 1QFD). Conserved residues are boxed in red. Similar residues are in black bold and boxed in yellow. α-helices are rendered as squiggles and strict β-turns as TT. Cysteine pairings for disulfide bridges are numbered as 1, 2 and 3. **d** Structure based sequence alignment of AhAI with other α-AIs. The sequences are as follows, α-AIs from A_hypochondriacus: *Amaranthus hypochondriacus* (UniProtKB accession ID: P80403), E_coracana: *Eleusine coracana* (UniProtKB accession ID: P01087), Z_mays; *Zea mays* (UniProtKB accession ID: P01088), W_religiosa: *Wrightia religiosa* (UniProtKB accession ID: V5W9K8), A_cathartica: *Allamanda cathartica* (UniProtKB accession ID: U5JE23), T_aestivum: *Triticum aestivum* (UniProtKB accession ID: P01085) and *Beta vulgaris* α-amylase inhibitor (GenBank accession No. XP_010672947.1). The figure was created using ESPript 3 program

was detected by western blot. GFP protein was detected in the apoplastic fluid of leaves infiltrated with AhAI signal peptide-GFP fused construct but was absent in cellular extract devoid of apoplastic content. Contrary, GFP protein was not detected in the apoplastic fluid of leaves infiltrated with only GFP construct but evident in remaining cellular extract (Fig. 4b and Fig. S2). Thus, these findings clearly demonstrated the involvement of AhAI signal peptide in the transport of attached protein to the extracellular space in plant cell.

AhAI is a potent inhibitor of coleopteran α-amylases

To evaluate the specific biochemical function, *AhAI* was heterologously expressed in the *E. coli* cells. Molecular weight of expressed protein was 13.2 kDa as determined by MALDI analysis (Fig. 5a). Inhibitory potential of recombinant AhAI (rAhAI) was evaluated against a wide range of α-amylases belonging to human, insect, fungi and bacteria (Fig. 5b). rAhAI was effective in complete inhibition of the amylolytic activity of coleopteran α-amylases i.e.

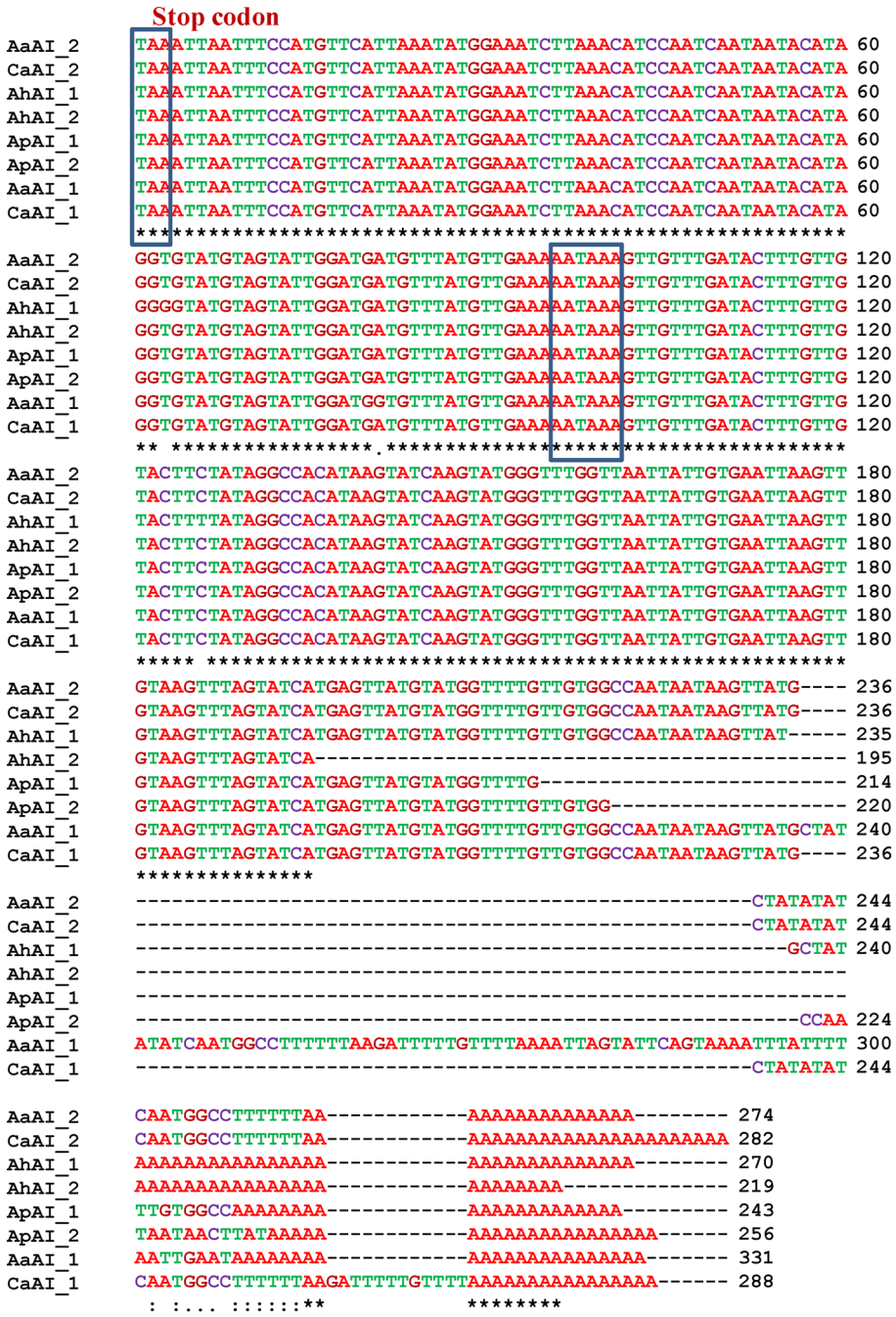

Fig. 2 3′ UTR variation within *AhAI* transcripts from four species of Amaranthaceae family. Nucleotide sequences of varied *AhAI* transcripts were aligned using ClustalW. Nucleotides A, T, G and C were colored in red, green, brick red and magenta respectively. A stop codon was boxed at the beginning of the alignment. Poly 'A' tailing signal was highlighted using the blue box. *Asterisk* '*' indicates identical residues, *Colon* ':' indicates conservation between groups and *period* '.' indicates conservation between dissimilar groups

crude α-amylases from adult *T. castaneum* and *C. chinensis* larvae. However, crude α-amylases from *T. castaneum* larvae and *C. chinensis* adults showed moderate inhibition (48 and 43%, respectively). Interestingly, the activity of human salivary α-amylase and crude α-amylases from adults and larvae of *H. armigera* were remained unaffected by rAhAI. Moreover, human pancreatic α-amylase and fungal α-amylase diastase showed moderate inhibition (38 and 50%, respectively) whereas purified α-amylase from *Bacillus licheniformis* showed only 15% inhibition by rAhAI. Potential of rAhAI to inhibit the amylolytic activity of recombinant lepidopteran and coleopteran α-amylases were also tested (Fig. 5c). Recombinant α-amylases from *T. castaneum* (TcAmy) and *C. chinensis* (CcAmy) showed complete inhibition while two recombinant α-amylases from *H. armigera* viz. HaAmy1and HaAmy2 showed complete resistance to inhibition even at a very high concentration of rAhAI (Fig. 5c).

Further, a concentration-dependent effect of rAhAI on growth and development of *C. chinensis* was evaluated. The effect was measured at a concentration of 10 and 25 µM of rAhAI and indicated as a means of relative adult

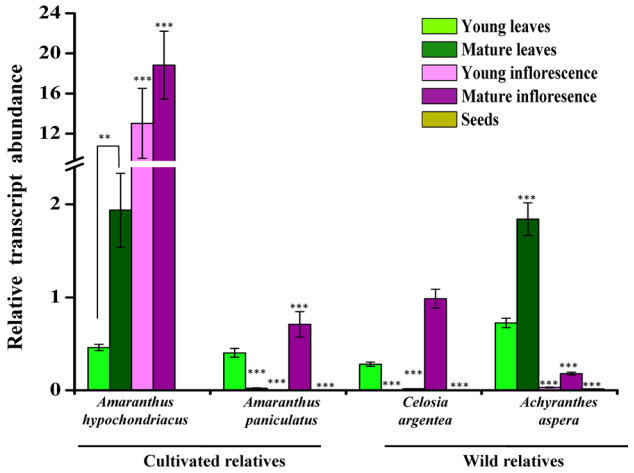

Fig. 3 *AhAI* transcript abundance across different plants tissues from Amaranthaceae family. *AhAI* transcript abundance was analyzed in different plant tissues viz. young leaves (*light green*), mature leaves (*dark green*), young inflorescence (*light pink*) and mature inflorescence (*dark pink*) using qPCR. Transcript abundance was compared between four species of Amaranthaceae family viz. *A. hypochondriacus, A. paniculatus, Celosia argentea* and *Achyranthes aspera*. Absolute quantification was carried out using the standard curve method with EF1α as a reference gene. In statistical analysis, one-way ANOVA was performed followed by Tukey's post hoc test. Statistical data is significant at *P*-value *** < 0.001 and ** < 0.01

emergence and average weight per emerged insect (Fig. 5d, e). Reduction in adult emergence was noted (40%) in rAhAI exposed insect as compared to the insect fed without inhibitor. Insect fed with 10 and 25 µM rAhAI showed relatively similar adult emergence. Further, the average weight for the insects fed with inhibitor was slightly higher than insect fed on control grains (without inhibitor). A similar increase in weight was also evident for *Leptinotarsa decemlineata, Psylliodes chrysocephala* and *Spodoptera littoralis* when fed with plant protease inhibitors (De Leo et al. 1998; Girard et al. 1998; Cloutier et al. 2000).

Differential interaction might be responsible for concentration-dependent inhibition of coleopteran α-amylases

Inhibitory activity of rAhAI was evaluated against recombinant TcAmy and CcAmy using a concentration range from 0 to 0.4 nM. Recombinant TcAmy was completely inhibited at 0.15 nM of rAhAI while 0.4 nM was required to inhibit rCcAmy (Fig. 6). This concentration-dependent differential inhibition of rAhAI against rTcAmy and rCcAmy was explained using molecular docking. An inhibitory loop of AhAI showed a similar conformational arrangement in the binding pockets of TcAmy and CcAmy except that Arg7 and Tyr28 made differential contacts with active site residues of both the enzymes

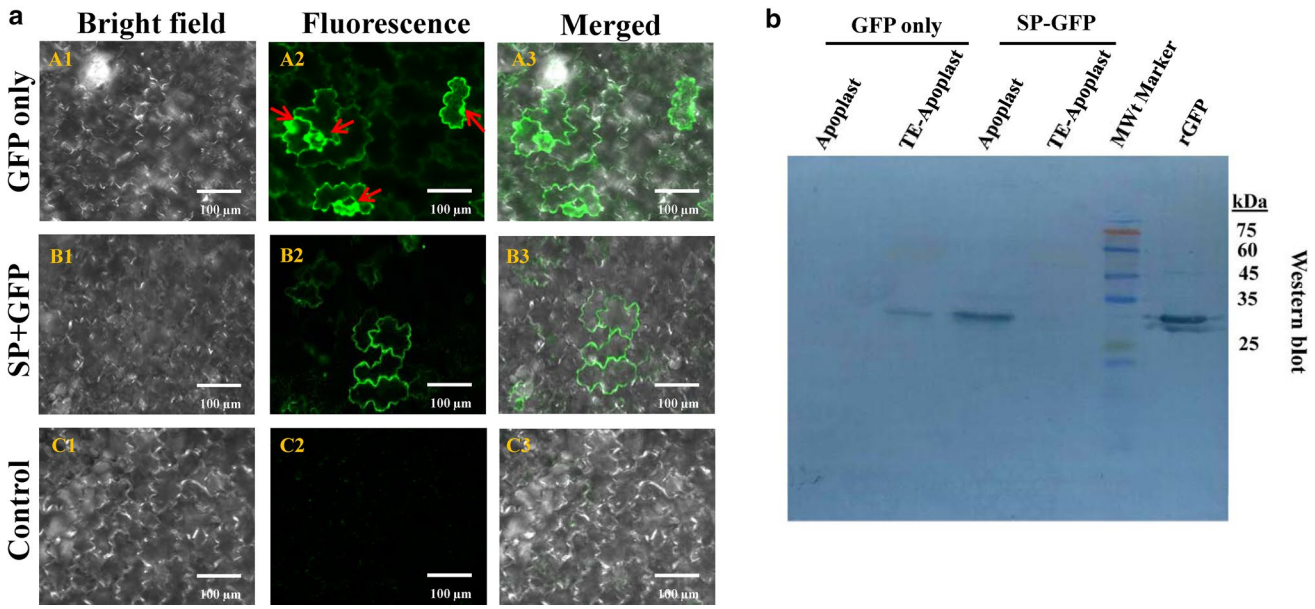

Fig. 4 Sub-cellular localization of GFP in absence and presence of *AhAI* signal peptide visualized in agro-infiltrated tobacco epidermal cells. **a** Images of agro-infiltrated tobacco epidermal cells using constructs pRI101-AN: GFP (A1–A3), pRI101-AN:SP-GFP (B1–B3) and only pRI101-AN (C1–C3) were taken at roughly 4 dpi. All images were taken in a single optical plane. *Arrowhead* points to the nucleus. The *last panel* shows merged images of bright and fluorescence fields. Scale represents 100 µm distance. Fluorescence in tobacco epidermal cells infiltrated with only GFP construct was seen mainly in nucleus and cytoplasm whereas for SP-GFP construct, it was mainly seen in apoplasts. **b** Detection of GFP protein (27 kDa) by western blot in apoplast and total cellular leaf extract devoid of apoplast. Recombinant GFP was used as a positive control in the last lane. '*TE*' represents total cellular leaf extract of tobacco leaves

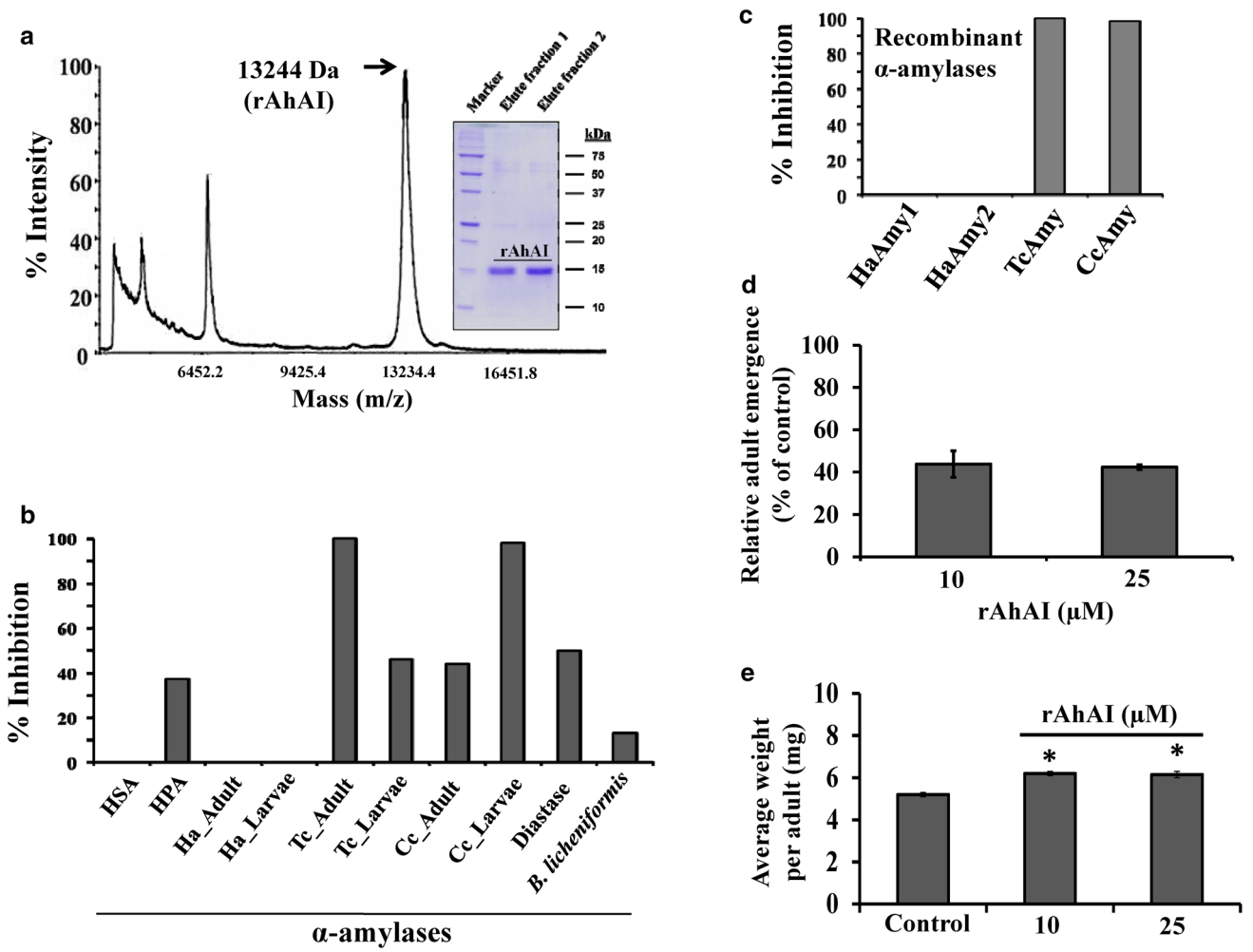

Fig. 5 Inhibitory activity of rAhAI against various α-amylases. **a** Acquisition of accurate molecular weight of rAhAI from mass spectrometric measurements. Inset SDS-PAGE image shows rAhAI fraction purified through Ni–NTA affinity column. **b** Inhibitory activity rAhAI against human salivary amylase (HSA), human pancreatic amylase (HPA), crude α-amylase from *Helicoverpa armigera* adults (Ha_Adult) and larvae (Ha_Larvae), crude α-amylase from *Tribolium castaneum* adults (Tc_Adult) and larvae (Tc_Larvae), crude α-amylase from *Callosobruchus chinensis* adults (Cc_Adult) and larvae (Cc_Larvae), α-amylase from fungal source i.e. diastase and α-amylase from bacteria *Bacillus licheniformis*. **c** Inhibitory activity of rAhAI against recombinant α-amylases viz. *H. armigera* α-amylase 1 and 2 (HaAmy1 and HaAmy2), *T. castaneum* α-amylase (TcAmy) and *C. chinensis* α-amylase (CcAmy). **d** and **e**. Effect of different concentrations of rAhAI on *C. chinensis* growth and development. One-way ANOVA was performed followed by Tukey's post hoc test. Statistical data is significant at *P*-value * < 0.005

(Fig. 6). In TcAmy, Arg7 alone made contact with two active site residues i.e. Asp187 and Glu224 and also with adjacent Tyr28 residue on the inhibitory loop. Tyr28 also formed hydrogen bond contact with TcAmy active site residue Asp187. In the case of CcAmy, Arg7 made a single contact with active site residues Asp286 and also with adjacent Tyr28 residue on the inhibitory loop. Tyr28 also formed hydrogen bond contact with enzymes active site residue Glu221. In TcAmy, aa residues from inhibitory loops formed three hydrogen bonds with active site residues from enzymes which might be energetically more favourable than two hydrogen bonds as observed between AhAI and CcAmy.

Discussion

Insect pests are the major threat to the economically important crops as they cause severe economic losses. α-amylases of the insect pests through digestion of starch play a key role in overall energy assimilation and metabolism. Plants, on the other hand, are equipped with various α-AIs to impede the growth of insect pests in order to mitigate the insect infestation. A 32 aa long proteinaceous α-AI from *A. hypochondriacus* was reported (Chagolla-Lopez et al. 1994). We cloned the complete DNA sequence of *AhAI*, which had typical three cysteine residues and one disulfide bond conserved within known α-AIs from eudicots

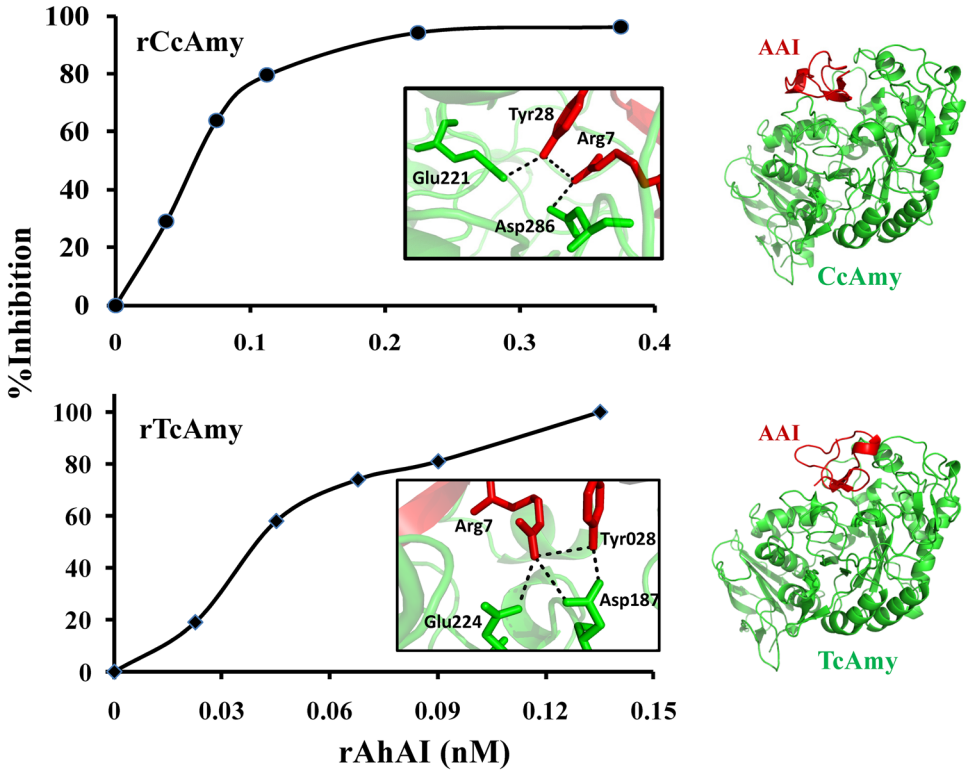

Fig. 6 Inhibitory potential of rAhAI against recombinant *T. castaneum* and *C. chinensis* α-amylases. 0.02–0.15 nM and 0.04–0.4 nM of rAhAI was tested for inhibitory activity against *T. castaneum* α-amylase (TcAmy) and *C. chinensis* α-amylase (CcAmy), respectively. Insight molecular docking figures highlight molecular interactions of rAhAI against both the α-amylases

and monocots (Chagolla-Lopez et al. 1994; Lu et al. 1999; Franco et al. 2002). Identical genomic and ORFs were characterized from four members of Amaranthaceae family having 26 aa signal peptide and 75 aa pro-peptide. However, 32 aa peptide alone shown to have inhibitory activity (Chagolla-Lopez et al. 1994; Lu et al. 1999). α-AI transcripts were differentially expressed in various plant tissues with the highest abundance in flowers. Fluorescent tag based sub-cellular localization revealed the role of AhAI signal peptide in extracellular secretion. Full-length 75 aa rAhAI revealed a wide range of inhibition against α-amylases. In vitro and in vivo studies suggested that rAhAI was efficient in inhibiting the amylolytic activity of two coleopteran insects. Further, insect feeding assays on mung bean seeds showed the potential of rAhAI in limiting overall development and adult emergence in the case of *C. chinensis*. On the other hand, rAhAI failed to inhibit *H. armigera* α-amylases as well as human salivary α-amylase.

When compared with other α-AIs from monocots and dicots, AhAI showed conserved α-helix and disulfide bond that are necessary to retain knottin fold and hence inhibitory activity. Native pre-protein consisted of the signal peptide and unprocessed protein (AhAI) which is a pro-form of previously reported 32 aa mature peptide. Proteolytic maturation was reported for many types of proteins including peptide hormones, digestive enzymes and coagulation proteins. Before entering to the vacuoles, many plant vacuolar proteins were processed to their C-terminal of Aspargine moiety by Asn-specific proteases (Hara-Nishimura et al. 1991). Similar activation of mature α-AI peptide from its pro-protein form towards carboxyl end of Asn was reported for *Phaseolus vulgaris* α-AI (Pueyo et al. 1993). Another related *P. vulgaris* α-AI (α-AI-2) was processed at particular Asn site to release α and β subunits which were assembled into its active heterodimer form. Such processing of pro-protein was predicted to remove conformational constraint and to produce a biochemically active form of the inhibitor (Pueyo et al. 1993; Nakaguchi et al. 1997). With respect to AhAI inhibitor, the similar Asn69 site was present at N'-terminus of the mature peptide. Processing of AhAI into 32 aa mature form was evident as only mature peptide was known to be derived in abundant quantity from *A. hypochondriacus* seeds (Chagolla-Lopez et al. 1994; Lu et al. 1999; Martins et al. 2001). Further, we found rAhAI containing 75 aa was biochemically active with contrast to the earlier prediction of the need for processing of pro-protein to become an active inhibitor of 32 aa. The sequence similarity and motif search for uncharacterized 43 aa peptide revealed that motifs present on this peptide are identical with those on proteins involved in sensing biological stress. Thus, this uncharacterized 43 aa peptide might be involved as stress sensor. As Asn specific pro-protein processing pathway is evolutionary active in *A. hypochondriacus* seeds, the presence of active α-AI protein (75 aa AhAI) suggested an additional advantage to the inhibitory function.

α-AIs with small variations in their primary structure exist in a few plants and their related species. For example, monomeric α-AIs with few nucleotide variations were present in wheat and aegilops which were thought to be evolved from common ancestral gene through duplication and mutation (Wang et al. 2008). Similarly, a higher diversity of α-AIs was present in wild accessions than cultivated accessions of common bean (Ishimoto et al. 1995). Hi-lysine barley mutants also showed higher accumulation of mRNA of BASI in seeds (Leah and Mundy 1989). Interestingly, in the present study, *AhAI* transcripts with identical ORF were observed in one cultivated and two wild relatives of *A. hypochondriacus viz. A. paniculatus, A. aspera* and *C. argentea*, respectively. Variation in expression of *AhAI* transcripts was observed across different tissues of the above-mentioned plants. In *A. hypochondriacus*, highest *AhAI* expression was observed in mature inflorescence which is an essential part for reproduction and requires more protection from insect attack before seeds mature. A similar variation of expression in α-AIs was also observed in wheat and its close relatives (Zoccatelli et al. 2012). Although for most wheat and barley *α-AI*s genes are expressed only during seed development and remained at an undetectable level in other plant tissues (Sanchez et al. 1994; Altenbach et al. 2011).

Variation in 3′UTR region is known to be responsible for regulation of translation of a particular transcript. We have sequenced various *AhAI* transcripts from *A. hypochondriacus* and related species to identify such variation only in 3′UTR region. 3′UTR regions of plant viral RNAs and mammalian RNAs have been studied extensively. However, 3′UTR region in plants has not been studied thoroughly for its regulatory role under different conditions as very few examples exist. For example, 3′ UTR region of invertase gene in maize was studied for its involvement in sensing carbon starvation (Cheng et al. 1999). In sweet cherry also, 3′UTR sequences were used as SNP and haplotype markers to improve plant genomic resources (Koepke et al. 2012). Further, polyadenylation sites in 3′UTR region were experimentally determined in plants by high-throughput sequencing which has revealed the great potential for regulation of plant gene expression (Ma et al. 2014). In the present study, we have identified conserved single polyadenylation site in 3′ UTR region of *AhAI* transcripts from all the four Amaranthaceae members. However, no other regulatory sites or secondary structure variations were observed on *AhAI* 3′UTR region and the molecular basis for polymorphism in 3′UTR remains unknown.

Analysis of *AhAI* transcript abundance in different plant tissues of *A. hypochondriacus* and related species indicated negligible expression of *AhAI* transcripts in mature seeds in spite of the fact that mature inhibitor peptide was reported abundantly from mature *A. hypochondriacus* seeds (Chagolla-Lopez et al. 1994). We hypothesize that protein produced in other parts of the plant was being transported to seeds. The appropriate signal sequence is required for effective transport of mature α-AI to seeds. Signal peptide composition in AhAI pre-protein showed charged N-terminal, central hydrophobic and polar C-terminal region which was in well accordance with other known eukaryotic signal peptides (Heijne 1985; Heijne and Abrahmsen 1989). Additionally, we clearly demonstrated the role of this signal peptide in an extracellular transport of attached protein in vivo. To our knowledge, this is the first report of in vivo functional characterization of the signal peptide from plant α-AI.

To become an effective α-AI, it should be able to inhibit α-amylases from a wide range of sources with minimal concentration and high specificity. In the present study, the potential of rAhAI to inhibit α-amylases from different sources showed distinct inhibition pattern. rAhAI indicated more specificity towards coleopteran α-amylases than lepidopteran, fungal, bacterial and mammalian α-amylases. Moderate inhibition was observed in the case of fungal and bacterial α-amylases. A similar differential inhibition with respect to insect and mammalian α-amylases was observed for rye α-AI (Lulek et al. 2000). Also, rAhAI had moderate inhibitory activity against human pancreatic α-amylase and was unable to inhibit human salivary α-amylase as well as α-amylases from *H. armigera*. Similar differential specificities were observed in interactions of wheat α-AI with human salivary and pancreatic α-amylase (O'connor and McGeeney 1981). Moreover, the variable inhibitory potential of common bean α-amylases was observed against coleopteran, hymenopteran and dipteran α-amylases (Kluh et al. 2005). Analogous interactions between enzyme-inhibitor complexes of bean α-AI with mammalian and *T. molitor* α-amylase (TMA) revealed deviations in the interacting inhibitory loop (Nahoum et al. 1999). Further, very low concentrations (nanomolar) of rAhAI were required for complete inhibition of *T. castaneum* and *C. chinensis* α-amylases. CcAmy required a relatively higher quantity of rAhAI than TcAmy for complete inhibition of amylolytic activity.

Molecular docking studies highlighted differential hydrogen bonding between active site residues of enzyme and Arg7 and Tyr28 residues of the inhibitory loop. AhAI upon binding with α-amylases adopted more compact conformation with increased intramolecular hydrogen bonding (Carugo et al. 2001; Micheelsen et al. 2008). Similar bonding was observed between Arg7 and Tyr28 of AhAI inhibitory loop after interactions with TcAmy and CcAmy. These interactions stabilized AhAI inhibitory loop over the active sites of the target α-amylases (Martins et al. 2001). Interaction of TMA with AhAI revealed that inhibitor bound to the active site groove of the enzyme by blocking substrate

entry site and central four sugar-binding sub-sites (Pereira et al. 1999). Arginine and tyrosine residues residing in the inhibitory loop of other α-AIs were imperative for these molecular interactions (Abe et al. 1993; Mirkov et al. 1995; Rodenburg et al. 1995). We identified analogous AhAI residues interacting with active site residues of TcAmy and CcAmy with the difference in their hydrogen bonding pattern. This could demonstrate the molecular basis for the concentration-dependent inhibition of AhAI to completely deactivate above coleopteran α-amylases.

Until now, the effectiveness of 32 aa α-AI in controlling insect pests growth and development has been studied by in vitro interactions of AhAI with purified insect digestive α-amylases. AhAI was found to be effective in inhibiting the amylolytic activity of α-amylases from a lepidopteran pest, *Tecia solanivora* (Valencia-Jimenez et al. 2008). Another report highlighted the potential of α-AI in inhibiting the amylolytic activity of α-amylases from coleopteran pests viz. *T. castaneum* and *Prostephanus truncates* (Chagolla-Lopez et al. 1994). However, this is the first report showing the effectiveness of 75 aa AhAI in mitigating growth and development of *C. chinensis*- a coleopteran pest by incorporating the inhibitor into the insect diet. Besides *AhAI*, various other α-AIs were expressed in host plants of insect pests and the efficacy was tested by performing insect feeding assays (Morton et al. 2000; De; Sousa-Majer et al. 2007; Barbosa et al. 2010; Luthi et al. 2013). In the present study, detailed genomic and functional analysis of *AhAI* suggested its potential in mitigating insect infestation. Generating transgenic plants expressing *rAhAI* would be the next step to evaluate the efficacy of the AhAI as an inhibitor in environment-friendly pest management efforts.

Acknowledgements AJB and SKR thank Council for Scientific and Industrial Research (CSIR) for Senior Research Fellowship and Dept. of Science and Technology (DST), New Delhi for Ramanujan Fellowship, respectively. Authors thanks Dt. Bhushan Dholakia for critically reading and providing suggestions in the manuscript drafts. This project is supported by the Department of Biotechnology, Goverment of India (BT/PR2295/AGR/5/552/2011) to CSIR-National Chemical Laboratory (GAP 298126), Pune, and North Maharashtra University, Jalgaon. This project is also supported by CSIR under XII five year plan projects (BSC0107 and BSC0120) to CSIR-National Chemical Laboratory, Pune.

Author contributions APG, SKR, PKP and VLM designed the experiments. AJB, SMC, and KB conducted the experiments. YY performed homology modelling and docking studies. AJB, VSG and APG wrote the manuscript. All authors read and approved the final manuscript.

Compliance with ethical standards

Conflict of interest The authors declare they have no conflicts of interest.

References

Abe J, Sidenius U, Svensson B (1993) Arginine is essential for the alpha-amylase inhibitory activity of the alpha-amylase/subtilisin inhibitor (BASI) from barley seeds. Biochem J 293:151–155

Altenbach SB, Vensel WH, Dupont FM (2011) The spectrum of low molecular weight alpha-amylase/protease inhibitor genes expressed in the US bread wheat cultivar Butte 86. BMC Res Notes 4:242

Ambekar SS, Patil SC, Giri AP, Kachole MS (1996) Proteinaceous inhibitors of trypsin and of amylases in developing and germinating seeds of pigeon pea (*Cajanus cajan* (L) Millsp). J Sci Food Agric 72:57–62

Barbosa AE, Albuquerque EV, Silva MC, Souza DS, Oliveira-Neto OB, Valencia A, Rocha TL, Grossi-de-Sa MF (2010) Alpha-amylase inhibitor-1 gene from *Phaseolus vulgaris* expressed in *Coffea arabica* plants inhibits alpha-amylases from the coffee berry borer pest. BMC Biotechnol 10:44

Bartel DP (2009) MicroRNAs: target recognition and regulatory functions. Cell 136:215–233

Bhide AJ, Channale SM, Patil SS, Gupta VS, Ramasamy S, Giri AP (2015) Biochemical, structural and functional diversity among *Helicoverpa armigera* amylases. Biochim Biophys Acta 1850:1719–1728

Carugo O, Lu S, Luo J, Gu X, Liang S, Strobl S, Pongor S (2001) Structural analysis of free and enzyme-bound amaranth alpha-amylase inhibitor: classification within the knottin fold superfamily and analysis of its functional flexibility. Protein Eng 14:639–646

Chagolla-Lopez A, Blanco-Labra A, Patthy A, Sánchez R, Pongor S (1994) Purified AAI strongly inhibits the alpha-amylase activity of insect larvae (*Tribolium castaneum* and *Prostephanus truncatus*) and does not inhibit proteases and mammalian alpha-amylases. J Biol Chem 269:23675–23680

Channale SM, Bhide AJ, Yadav Y, Kashyap G, Pawar PK, Maheshwari VL, Ramasamy S, Giri AP (2016) Characterization of two coleopteran a-amylases and molecular insights into their differential inhibition by synthetic α-amylase inhibitor, acarbose. Insect Biochem Mol Biol 74:1–11

Cheng WH, Taliercio EW, Chourey PS (1999) Sugars modulate an unusual mode of control of the cell-wall invertase gene (Incw1) through its 3′ untranslated region in a cell suspension culture of maize. Proc Natl Acad Sci USA 96:10512–10517

Cloutier C, Jean C, Fournier M, Yelle S, Michaud D (2000) Adult Colorado potato beetles, *Leptinotarsa decemlineata* compensate for nutritional stress on oryzacystatin I-transgenic potato plants by hypertrophic behavior and over-production of insensitive proteases. Arch Insect Biochem Physiol 44:69–81

Dayler CS, Mendes PA, Prates MV, Bloch C Jr, Franco OL, Grossi-de-Sá MF (2005) Identification of a novel bean alpha-amylase inhibitor with chitinolytic activity. FEBS Lett 579:5616–5620

De Leo F, Bonade-Bottino MA, Ceci LR, Gallerani R, Jouanin L (1998) Opposite effects on *Spodoptera littoralis* larvae of high expression level of a trypsin proteinase inhibitor in transgenic plants. Plant Physiol 118:997–1004

de Sousa-Majer MJ, Hardie DC, Turner NC, Higgins TJ (2007) Bean alpha-amylase inhibitors in transgenic peas inhibit development of pea weevil larvae. J Econ Entomol 100:1416–1422

Do Nascimento VV, Castro HC, Abreu PA, Oliveira AE, Fernandez JH, Araújo Jda S, Machado OL (2011) In silico structural characteristics and α-amylase inhibitory properties of Ric c 1 and Ric c 3, allergenic 2 S albumins from *Ricinus communis* seeds. J Agric Food Chem 59:4814–4821

Franco AL, Rigden DJ, Melo FR, Grossi-de-sa MF (2002) Plant α-amylase inhibitors and their interaction with insect α-amylases. Eur J Biochem 269:397–412

Girard C, Le Metayer M, Zaccomer B, Bartlet E, Williams I, Bonadé-Bottino M, Pham-Delegue M, Jouanin L (1998) Growth stimulation of beetle larvae reared on a transgenic oilseed rape expressing a cysteine proteinase inhibitor. J Insect Physiol 44:263–270

Giri AP, Kachole MS (1998) Amylase inhibitors of pigeonpea (*Cajanus cajan*) seeds. Phytochemistry 47:197–202

Giri AP, Chougule NP, Telang MA, Gupta VS (2004) Engineering insect tolerant plants using plant defensive proteinase inhibitors. Recent Dev Phytochem 8:117–137

Giri AP, Bhide AJ, Gupta VS (2016) Targeting digestive physiology: trends in strategic exploitation of plant defensive proteinaceous inhibitors against insect pests. Genetic engineering of plants–enhancing productivity and product value. John Wiley & Sons Limited, The Atrium, Southern Gate, Chichester

Gomez L, Sanchez-Monge R, Garcia-Olmedo F, Salcedo G (1989) Wheat tetrameric inhibitors of insect alpha-amylases: Alloploid heterosis at the molecular level. Proc Natl Acad Sci USA 86:3242–3246

Hara-Nishimura I, Inoue K, Nishimura M (1991) A unique vacuolar processing enzyme responsible for conversion of several proprotein precursors into the mature forms. FEBS Lett 294:89–93

Ishimoto M, Suzuki K, Iwanaga M, Kikuchi F, Kitamura K (1995) Variation of seed α-amylase inhibitors in the common bean. Theor Appl Genet 90:425–429

Kluh I, Horn M, Hýblová J, Hubert J, Dolecková-Maresová L, Voburka Z, Kudlíková I, Kocourek F, Mares M (2005) Inhibitory specificity and insecticidal selectivity of alpha-amylase inhibitor from *Phaseolus vulgaris*. Phytochemistry 66:31–39

Koepke T, Schaeffer S, Krishnan V, Jiwan D, Harper A, Whiting M, Oraguzie N, Dhingra A (2012) Rapid gene-based SNP and haplotype marker development in non-model eukaryotes using 3′UTR sequencing. BMC Genom 1186:1471–2164

Lagarda-Diaz I, Geiser D, Guzman-Partida AM, Winzerling J, Vazquez-Moreno L (2014) Recognition and binding of the PF2 lectin to α-amylase from *Zabrotes subfasciatus* (Coleoptera:Bruchidae) larval midgut. J Insect Sci 14:204

Lazaro A, Rodriguez-Palenzuela P, Maraña C, Carbonero P, Garcia-Olmedo F (1988) Signal peptide homology between the sweet protein thaumatin II and unrelated cereal alpha-amylase/trypsin inhibitors. FEBS Lett 239:147–150

Leah R, Mundy J (1989) The bifunctional α-amylase/subtilisin inhibitor of barley: nucleotide sequence and patterns of seed-specific expression. Plant Mol Biol 12:673–682

Limure T, Kihara M, Sato K, Ogushi K (2015) Purification of barley dimeric α-amylase inhibitor-1 (BDAI-1) and avenin-like protein-a (ALP) from beer and their impact on beer foam stability. Food Chem 172:257–264

Lin KF, Lee TR, Tsai PH, Hsu MP, Chen CS, Lyu PC (2007) Structure-based protein engineering for alpha-amylase inhibitory activity of plant defensin. Proteins 68:530–540

Liu YJ, Cheng CS, Lai SM, Hsu MP, Chen CS, Lyu PC (2006) Solution structure of the plant defensin VrD1 from mung bean and its possible role in insecticidal activity against bruchids. Proteins 63:777–786

Lovell SC, Davis IW, Arendall WB, de Bakker PI, Word JM, Prisant MG, Richardson JS, Richardson DC (2003) Structure validation by Cα geometry: ϕ, ψ and Cβ deviation. Proteins 50:437–450

Lu S, Deng P, Liu X, Luo J, Han R, Gu X, Liang S, Wang X, Li F, Lozanov V, Patthy A, Pongor S (1999) Solution structure of the major α-amylase inhibitor of the crop plant Amaranth. J Biol Chem 274: 20473–20478

Lulek J, Franco OL, Silva M, Slivinski CT, Bloch C Jr, Rigden DJ, Grossi de Sá MF (2000) Purification, biochemical characterisation and partial primary structure of a new alpha-amylase inhibitor from *Secale cereale* (rye). Int J Biochem Cell Biol 32:1195–1204

Lüthi C, Alvarez-Alfageme F, Ehlers JD, Higgins TJ, Romeis J (2013) Resistance of αAI-1 transgenic chickpea (*Cicer arietinum*) and cowpea (*Vigna unguiculata*) dry grains to bruchid beetles (Coleoptera: Chrysomelidae). Bull Entomol Res 103:373–381

Ma L, Pati PK, Liu M, Li QQ, Hunt AG (2014) High throughput characterizations of poly(A) site choice in plants. Methods 67:74–83

Martins JC, Enassar M, Willem R, Wieruzeski JM, Lippens G, Wodak SJ (2001) Solution structure of the main alpha-amylase inhibitor from amaranth seeds. Eur J Biochem 268:2379–2389

Micheelsen PO, Vévodová J, De Maria L, Ostergaard PR, Friis EP, Wilson K, Skjøt M (2008) Structural and mutational analyses of the interaction between the barley alpha-amylase/subtilisin inhibitor and the subtilisin savinase reveal a novel mode of inhibition. J Mol Biol 380:681–690

Mirkov TE, Evans SV, Wahlstrom J, Gomez L, Young NM, Chrispeels MJ (1995) Location of the active site of the bean alpha-amylase inhibitor and involvement of a Trp, Arg, Tyr triad. Glycobiology 5:45–50

Mishra M, Mahajan N, Tamhane VA, Kulkarni MJ, Baldwin IT, Gupta VS, Giri AP (2012) Stress inducible proteinase inhibitor diversity in *Capsicum annuum*. BMC Plant Biol 12:217

Morton RL, Schroeder HE, Bateman KS, Chrispeels MJ, Armstrong E, Higgins TJ (2000) Bean alpha-amylase inhibitor 1 in transgenic peas (*Pisum sativum*) provides complete protection from pea weevil (*Bruchus pisorum*) under field conditions. Proc Natl Acad Sci USA 97:3820–3825

Nahoum V, Farisei F, Le-Berre-Anton V, Egloff MP, Rougé P, Poerio E, Payan F (1999) A plant-seed inhibitor of two classes of alpha-amylases: X-ray analysis of Tenebrio molitor larvae alpha-amylase in complex with the bean *Phaseolus vulgaris* inhibitor. Acta Crystallogr D 55:360–372

Nakaguchi T, Arakawa T, Philo JS, Wen J, Ishimoto M, Yamaguchi H (1997) Structural characterization of an alpha-amylase inhibitor from a wild common bean (*Phaseolus vulgaris*): insight into the common structural features of leguminous alpha-amylase inhibitors. J Biochem 121:350–354

Napoleão TH, Pontual EV, de Albuquerque Lima T, de Lima Santos ND, Sá RA, Coelho LC, do Amaral Ferraz Navarro DM, Paiva PM (2012) Effect of *Myracrodruon urundeuva* leaf lectin on survival and digestive enzymes of *Aedes aegypti* larvae. Parasitol Res 110:609–616

Nguyen PQ, Wang S, Kumar A, Yap LJ, Luu TT, Lescar J, Tam JP (2014) Discovery and characterization of pseudocyclic cystine-knot α-amylase inhibitors with high resistance to heat and proteolytic degradation. FEBS J 281:4351–4366

O'Connor CM, McGeeney KF (1981) Isolation and characterization of four inhibitors from wheat flour which display differential inhibition specificities for human salivary and human pancreatic alpha-amylases. Biochim Biophys Acta 658:387–396

O'Leary BM, Rico A, McCraw S, Fones HN, Preston GM (2014) The infiltration-centrifuge technique for extraction of apoplastic fluid from plant leaves using *Phaseolus vulgaris* as an example. J Vis Exp 94:e52113. doi:10.3791/52113

Oganesyan N, Kim S, Kim R (2005) On-column protein refolding for crystallization. J Strct Funct Genom 6:177–182

Paes NS, Gerhardt IR, Coutinho MV, Yokoyama M, Santana E, Harris N, Chrispeels MJ, Grossi de Sa MF (2000) The effect of arcelin-1 on the structure of the midgut of bruchid larvae and immunolocalization of the arcelin protein. J Insect Physiol 46:393–402

Pereira PJ, Lozanov V, Patthy A, Huber R, Bode W, Pongor S, Strobl S (1999) Specific inhibition of insect alpha-amylases: yellow meal worm alpha-amylase in complex with the amaranth alpha-amylase inhibitor at 2.0 A resolution. Structure 7:1079–1088

Petrucci T, Rab A, Tomasi M, Silano V (1976) Further characterization studies of the alpha-amylase protein inhibitor of gel electrophoretic mobility 0.19 from the wheat kernel. Biochim Biophys Acta 420:288–297

Pueyo JJ, Hunt DC, Chrispeels MJ (1993) Activation of bean (*Phaseolus vulgaris*) alpha-amylase inhibitor requires proteolytic processing of the proprotein. Plant Physiol 101:1341–1348

Robert X, Gouet P (2014) Deciphering key features in protein structures with the new ENDscript server. Nucl Acids Res 42:320–324

Robertson M, Walker-Simmons M, Munro D, Hill RD (1989) Induction of alpha-amylase inhibitor synthesis in barley embryos and young seedlings by abscisic acid and dehydration stress. Plant Physiol 91:415–420

Rodenburg KW, Várallyay E, Svendsen I, Svensson B (1995) Arg-27, Arg-127 and Arg-155 in the beta-trefoil protein barley alpha-amylase/subtilisin inhibitor are interface residues in the complex with barley alpha-amylase 2. Biochem J 309:969–976

Sali A, Blundell TL (1993) Comparative protein modelling by satisfaction of spatial restraints. J Mol Biol 234:779–815

Sanchez de la Hoz P, Castagnaro A, Carbonero P (1994) Sharp divergence between wheat and barley at loci encoding novel members of the trypsin/alpha-amylase inhibitors family. Plant Mol Biol 26:1231–1236

Sanchez-Monge R, Gomez L, Garcia-Olmedo F, Salcedo G (1986) A tetrameric inhibitor of insect alpha-amylase from barley. FEBS Letters 207(1):105–109

Sarate PJ, Tamhane VA, Kotkar HM, Ratnakaran N, Susane N, Gupta VS, Giri AP (2012) Developmental and digestive flexibilities in the midgut of polyphagous insect, the cotton bollworm, *Helicoverpa armigera*. J Insect Sci 12:42

Shi ZD, Qian XM, Zhang JX, Han L, Zhang KL, Chen LY, Zhou X, Zhang JN, Kang CS (2014) BASI, a potent small molecular inhibitor, inhibits glioblastoma progression by targeting microRNA-mediated β-catenin signaling. CNS Neurosci Ther 20(9):830–839

Strobl S, Maskos K, Wiegand G, Huber R, Gomis-Rüth FX, Glockshuber R (1998) A novel strategy for inhibition of alpha-amylases: yellow meal worm alpha-amylase in complex with the Ragi bifunctional inhibitor at 2.5 A resolution. Structure 6:911–921

Tamura K, Stecher G, Peterson D, Filipski A, Kumar S (2013) MEGA 6: molecular evolutionary genetics analysis version 6.0. Mol Biol Evol 30:2725–2729

Tovchigrechko A, Vakser IA (2006) GRAMM-X public web server for protein-protein docking. Nucleic Acids Res 34:310–324

Valencia-Jiménez A, Arboleda JW, López Avila A, Grossi-de-Sá MF (2008) Digestive alpha-amylases from *Tecia solanivora* larvae (Lepidoptera: Gelechiidae): response to pH, temperature and plant amylase inhibitors. Bull Entomol Res 98:575–579

Vallée F, Kadziola A, Bourne Y, Juy M, Rodenburg KW, Svensson B, Haser R (1998) Barley alpha-amylase bound to its endogenous protein inhibitor BASI: crystal structure of the complex at 1.9 A resolution. Structure 6:649–659

Vijayan S, Imani J, Tanneeru K, Guruprasad L, Kogel KH, Kirti PB (2012) Enhanced antifungal and insect α-amylase inhibitory activities of Alpha-TvD1, a peptide variant of *Tephrosia villosa* defensin (TvD1) generated through in vitro mutagenesis. Peptides 33:220–229

von Heijne G (1985) Signal sequences: the limits of variation. J Mol Biol 184:99–105

von Heijne G, Abrahmsen L (1989) Species-specific variation in signal peptide design Implications for protein secretion in foreign hosts. FEBS Lett 244:439–446

Wang JR, Wei YM, Yan ZH, Zheng YL (2008) SNP and haplotype identification of the wheat monomeric alpha-amylase inhibitor genes. Genetica 134:277–285

Webb B, Sali A (2014) Comparative protein structure modeling using MODELLER. Curr Protoc Bioinform 47:1–32

Wiegand G, Epp O, Huber R (1995) The crystal structure of porcine pancreatic alpha-amylase in complex with the microbial inhibitor Tendamistat. J Mol Biol 247:99–110

Wisessing A, Engkagul A, Wongpiyasatid A, Choowongkomon K (2010) Biochemical characterization of the alpha-amylase inhibitor in mung beans and its application in inhibiting the growth of *Callosobruchus maculatus*. J Agric Food Chem 58:2131–2137

Yamasaki T, Deguchi M, Fujimoto T, Masumura T, Uno T, Kanamaru K, Yamagata H (2006) Rice bifunctional alpha-amylase/subtilisin inhibitor: cloning and characterization of the recombinant inhibitor expressed in *Escherichia coli*. Biosci Biotechnol Biochem 70:1200–1219

Zavala JA, Giri AP, Jongsma MA, Baldwin IT (2008) Digestive duet: midgut digestive proteinases of *Manduca sexta* ingesting *Nicotiana attenuata* with manipulated trypsin proteinase inhibitor expression. Plos ONE 3:e2008.

Zoccatelli G, Sega M, Bolla M, Cecconi D, Vaccino P, Rizzi C, Chignola R, Brandolini A (2012) Expression of α-amylase inhibitors in diploid Triticum species. Food Chem 135:2643–2649